

Ensemble Results of Solute Transport in 2D Operator-Stable Random Fields

Nathan Monnig, David Benson

Colorado School of Mines, nmonnig@mines.edu, dbenson@mines.edu, Golden, CO, USA

ABSTRACT

As it moves through an aquifer, a dissolved solute plume will evolve according to the complex heterogeneities that are present at many scales. Some statistical model must account for the aquifer structure. A fractional Brownian motion (fBm) model has been shown to create the long-range correlation that can produce continually faster-than-Fickian plume growth. Previous fBm models have assumed isotropic scaling (defined by a scalar Hurst coefficient). Motivated by field measurements, recent techniques were developed to handle anisotropic scaling, in which the scaling, or self-similarity parameter, is defined by a matrix. Ensemble numerical results are analyzed for solute transport through some of these 2D operator-stable fBm fields. Both the longitudinal and transverse Hurst coefficients are important in solute transport. Smaller Hurst coefficients in the transverse direction lead to more stretching of the convolution kernel in the direction of transport. This stretching creates a more stratified aquifer, with more continuity in high and low values in hydraulic conductivity (K). The result is faster-than-Fickian growth rates, and a longer tail in the breakthrough curve.

INTRODUCTION

In the past two decades, many researchers have investigated contaminant transport in fractional Brownian motion (fBm) and fractional Gaussian noise (fGn) random hydraulic conductivity (K) fields. Both numerical solutions and analytic approximations have been explored. Due to the rapid advance of computational power, numerical models can now be created in multiple dimensions on much larger and more realistic scales. Here we investigate Monte Carlo simulation of solute transport through 2-dimensional (2D) fBm fields.

Fractional Brownian motion is an intriguing model for aquifer hydraulic conductivity because it allows for evolving heterogeneity at all scales, typical of many real-world data sets. An fBm model can create the long-range dependence structures that are often observed in aquifers. Previous applications of fBm models to groundwater flow have assumed isotropic scaling in which the fBm is defined by a single, scalar Hurst coefficient. Isotropic scaling is an unrealistic assumption for granular sedimentary aquifers—it is likely that there is greater correlation in the horizontal and/or dip direction compared to the strike or vertical directions. In hydrogeologic systems it is typical to assume anisotropy in aquifer parameters, e.g., the dispersivity tensor. Indeed, many studies have presented evidence of anisotropic scaling in real-world aquifers [e.g. *Lui et al.*, 1997; *Castle et al.*, 2004]. Recently, improved techniques have been developed to handle anisotropic scaling [e.g. *Mason and Xiao*, 2001; *Benson et al.*, 2006].

Benson et al. [2006] presented a generalization of classic isotropic fBm that both allowed for anisotropic scaling as well as varying degrees of directional continuity in the K structure. This continuity can be defined by a probability measure on the unit circle in 2D, or the unit sphere in 3D. This “mixing measure” or weight function has the potential to model directionality that may be closely related to depositional patterns.

Benson et al. [2006] applied this mixing measure to a function $\phi(\mathbf{k})$, the convolution kernel in Fourier space. It is unclear exactly how this angular dependence in Fourier space corresponds to the true angular dependence in real space. In order to avoid uncertainty, we now apply the mixing measure directly to the function $\phi(\mathbf{x})$, the convolution kernel in real space. In this way the effect on the directionality in K -structure is clear. Additionally, *Benson et al.* [2006] presented the results of solute transport through single realizations of operator-scaling random fields, in order to compare directly between realizations with slightly different structure. However, their results cannot be translated to the “universal” behavior of the ensemble mean transport. Ensemble results are presented for all examples in this paper, making all results more robust.

The fields used in this study have two advantages over classical, isotropic fBm fields: (1) the operator-scaling fields are described by matrix scaling values which allow different scaling (or different Hurst coefficients) in different directions and (2) the mixing measure $M(\theta)$ is user-defined according to any

discretization by $\Delta\theta$ on the unit circle, allowing completely user defined directionality in K -structure. The fast Fourier transform (FFT) method is used, allowing rapid generation of large fBm fields.

1. Mathematical Background

Here we list a brief overview of the generation of operator-stable random fields. *Benson et al.* [2006] list a more rigorous derivation of the mathematical properties of multidimensional fBm. An isotropic fBm can be created by applying a Fourier filter with the scaling properties $\varphi(c\mathbf{k}) = c^{-A}\varphi(\mathbf{k})$ to a Gaussian white noise in the spectral representation. The order of integration, A , is related to the Hurst coefficient, H , by $A = H + \frac{d}{2}$, with $0 < H < 1$ in d dimensions [*Benson et al.*, 2006]. In the anisotropic case, the scaling property is defined by the matrix power $c^{\mathbf{Q}}$: $\varphi(c^{\mathbf{Q}}\mathbf{k}) = c^{-A}\varphi(\mathbf{k})$. The matrix \mathbf{Q} defines the deviation from the isotropic case ($\mathbf{Q} = \text{diag}(1,1)$) [*Benson et al.*, 2006]. The scaling relation for the convolution kernel in real space can be derived from the scaling relation in Fourier space [*Benson et al.*, 2006]. The result (for diagonal matrix \mathbf{Q}):

$$\varphi(c^{\mathbf{Q}}\mathbf{x}) = c^A \left| c^{-\mathbf{Q}} \right| \varphi(\mathbf{x}) = c^{H+d/2+\text{tr}(\mathbf{Q})} \varphi(\mathbf{x}) \quad 1$$

For simplicity, in this paper we present operator-stable fields with orthogonal eigenvectors (diagonal matrix \mathbf{Q}), although this is not a requirement. A simple 2D convolution kernel that satisfies this scaling relation is:

$$\varphi(\mathbf{x}) = M(\theta) \left[|x_1|^{2/a_1} + |x_2|^{2/a_2} \right]^{(H+d/2-a_1-a_2)/2} \quad 2$$

where a_1 and a_2 are the diagonal components of \mathbf{Q} , and $M(\theta)$ is a measure of the directional weight, which is user-defined on the unit circle.

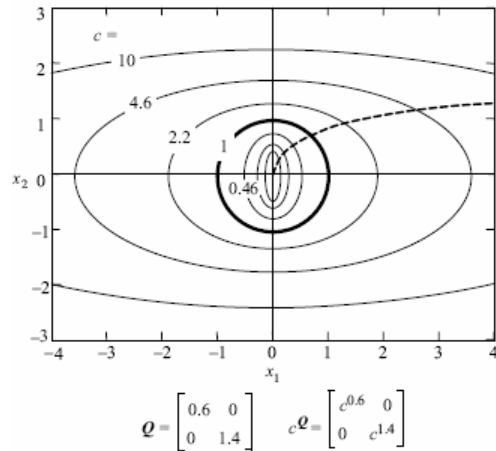


Figure 1. Matrix stretching of the points along the 45 degree angle according to the matrix $c^{\mathbf{Q}}$ which defines the deviation from the isotropic case $\mathbf{Q}=\text{diag}(1,1)$ (from *Benson et al.*, [2006]). Mathematically,

$$(x_1, x_2) = c^{\mathbf{Q}} \left(\frac{1}{\sqrt{2}}, \frac{1}{\sqrt{2}} \right) \text{ for all } c \geq 0.$$

2. Matrix Stretching

For any non-isotropic case (\mathbf{Q} is not the identity matrix $\text{diag}(1,1)$), the random process is distributionally self-similar along curves in space (except when sampling along the eigenvectors). Any straight lines between the eigenvectors will not follow the same power law and the Hurst coefficient will change [*Benson et al.*, 2006]. For this reason, the directional weights $M(\theta)$ must be stretched anisotropically according to the matrix \mathbf{Q} (Figure 1). This relation allows the tracing of angular sections of the unit circle that define the mixing measure into a “stretched” space defined by the operator-scaling relationship.

3. Fast Fourier Transform Convolution

Numerical evaluation of a convolution integral in multiple dimensions is, in general, very computationally intensive. For this reason, we make use of the theorem:

$$F^{-1}[F(f)F(g)] = f * g \quad 3$$

For functions f and g , and Fourier transform F , and inverse transform F^{-1} . In our case, the functions f and g are a Gaussian white noise, and the convolution kernel in real space (equation 2).

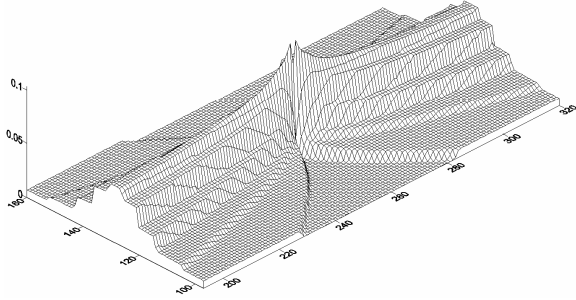


Figure 2. Example of convolution kernel with anisotropic mixing measure and anisotropic deviation matrix Q . ($H_{horiz} = 0.8$, $H_{vert} = 0.7$, mixing measure ranges from value of 0.12 in horizontal direction to 0 in vertical direction—refer to Benson et al. 2006, “braided” measure).

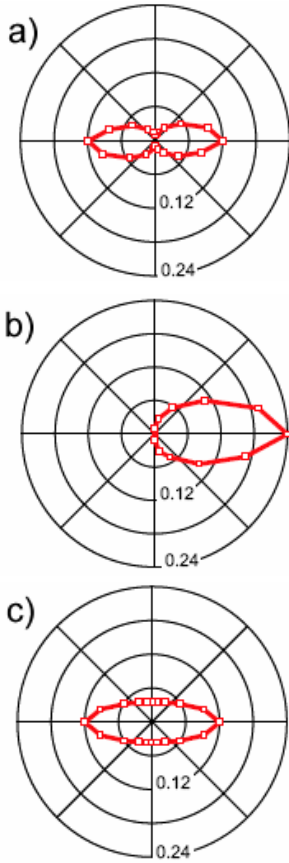


Figure 3. Anisotropic mixing measures presented in Benson et al. [2006] a.) “braided” b.) “downstream” c.) “elliptical”. $M(\theta)$, is discretized into 20 sections on the unit circle.

4. Results: Effects of the mixing measure

For all ensemble simulations presented, 50 realizations were compiled, each with a different “random” input Gaussian noise. The 2D input noise and the convolution kernel are 2048 by 1024 arrays. Both the noise and the kernel are transformed via FFT, multiplied together, then inverse FFT’ed to create the convolution as described in section 3. The middle 1/4 of each field is removed for transport simulation (avoiding wrap-around effects from the FFT) leaving a field with dimensions 1024 by 512 feet. MODFLOW is used to solve for the velocity field assuming an average hydraulic gradient across the fields of .01, with no-flow boundaries at the top and bottom of the field. In each realization 100,000 particles are released at time $t = 0$, spaced evenly between point 128 and 384 along the high head side of the fields (giving a total of 5,000,000 particles for each

ensemble of 50 realizations). No local dispersivity was used; Benson et al. [2006] found the effects of small local dispersivities to be insignificant in similar simulations.

To explore the effects of the mixing measure, or weight function $M(\theta)$, ensemble simulations were run with 2D random fields. Typical values of the Hurst coefficients from the literature were used: 0.5 in the horizontal (direction of transport) and 0.3 in the vertical or transverse direction. The fields were adjusted to be lognormally distributed with mean $\ln(K)=0$ and $\ln(K)$ variance=1.5. Ensemble results for the “braided”, “downstream”, “elliptical”, (see Figure 3) and isotropic measures were compared. The effects of these mixing measures are minimal. The braided and downstream measures create K -fields with continuity that resembles the braided stream which is the origin for the measure. The elliptical measure produces a somewhat smoother continuity in the hydraulic conductivity field. The isotropic measure is the only one that produces a significantly different K -field—a result of the much greater weight in the transverse direction. The breakthrough curves for all but the isotropic case are nearly indistinguishable. The breakthrough for the isotropic measure occurs later, due to less longitudinal continuity in the high and low- K zones.

5. Results: Variation of Transverse Hurst Coefficient

Benson et al. [2006] observed that higher orders of transverse integration create more vertical structure and increased layering in the aquifer. This leads to nearly Mercado-type plume growth. There is more persistence in high and low K material, which leads to more mass in the leading and trailing edges of the plume. The results of the present analysis are nearly the opposite. In Figure 4 we show sample realizations of K -fields with varying transverse Hurst coefficients.

The controlling parameter when the transverse Hurst coefficient is varied is the matrix stretching of the mixing measure. The lower the Hurst coefficient is in the vertical (with respect to the horizontal) the more stretching occurs in the horizontal direction. This stretching concentrates the weight in the convolution kernel closely along the horizontal axis. Lower orders of vertical integration produce much more stratified aquifers with more persistence in high and low K material,

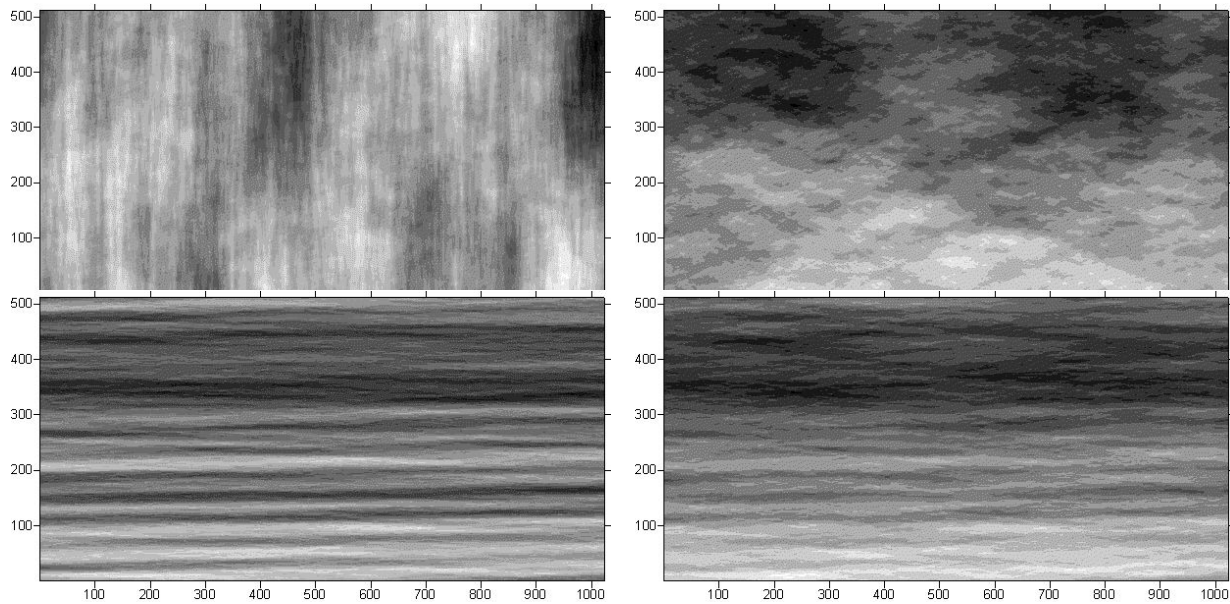


Figure 4. Log(K) plots showing the effect of different transverse Hurst coefficients. An identical input random noise was used in each convolution. Braided measure; starting from top left, moving clockwise: $H_{vert} = 0.7, 0.5, 0.3, 0.1$; $H_{horiz} = 0.5$.

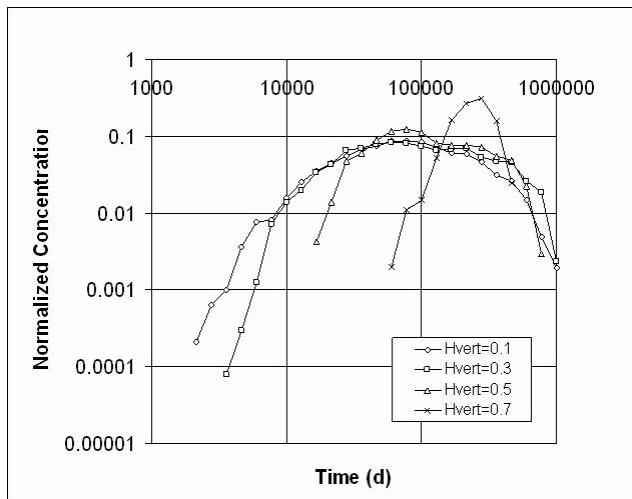


Figure 5. Normalized breakthrough curves at boundary $x=1024$ ft. for variation of transverse Hurst coefficient.

Figure 5) as well as faster plume growth. The early breakthrough for the lowest order of vertical integration occurs more than an order of magnitude before the early breakthrough for the highest order of vertical integration.

6. Comparison with Analytic Predictions

Neuman [1995], Rajaram and Gelhar [1995], and Di Federico and Neuman [1998] predict the spreading of plumes in isotropic fractal K -fields similar to those in our experiments. Their predictions are based only on the Hurst coefficient in the longitudinal direction. *Di Federico and Neuman [1998]* predict that a plume traveling in a fractal field with no fractal cutoff will exhibit permanently pre-asymptotic growth,

similar to the results *Benson et al. [2006]* describe for higher orders of integration in the transverse direction. This discrepancy may have to do with the fact that *Benson et al. [2006]* applied the stretched mixing measure to the convolution kernel in Fourier space while it is applied here to the convolution kernel in real space. It is unclear how directionality in Fourier space will manifest itself in real space. Thus, it is most logical to apply the mixing measure in real space.

In Figure 4 the effects of the matrix stretching are very clear. For $H_{vert} = 0.1$ and 0.3 , horizontal stretching producing strong continuity in the longitudinal direction. For $H_{vert} = H_{horiz} = 0.5$ we can see linear effects from the un-stretched discretization of the mixing measure. For $H_{vert} = 0.7$ we see continuity in the vertical direction due to the stretching in the transverse direction. This case, where $H_{vert} > H_{horiz}$ appears to be very unrealistic. Lower orders of integration in the vertical direction lead to earlier breakthrough (see

with a longitudinal macrodispersivity (α_L) that evolves according to $\alpha_L \propto \bar{X}^{1+2H}$ for mean travel distance \bar{X} and longitudinal Hurst coefficient H . *Rajaram and Gelhar* [1995] predict that plume growth in an fBm K -field will exhibit a macrodispersivity according to $\alpha_L \propto \bar{X}^H$ from a two-particle, relative dispersion approach. *Di Federico and Neuman* predict that if the plume growth exceeds the fractal cutoff (the plume is no longer continually sampling larger scales of heterogeneity) then there will be a transition to a Fickian growth rate ($\alpha_L = \text{const.}$). *Mercado* [1967] describes a perfectly stratified model with no mixing. This ballistic motion will exhibit linear growth of macrodispersivity versus travel distance ($\alpha_L \propto \bar{X}^H$). All of the above predictions are included in Figure 6.

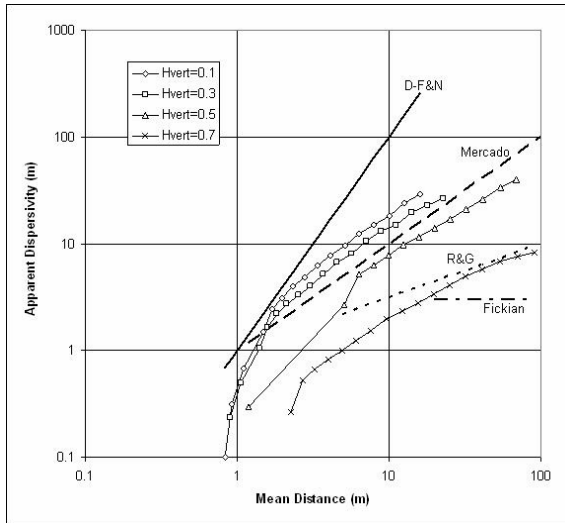


Figure 6. Apparent dispersivity vs. mean travel distance for ensemble plumes with different transverse H . Predictions for transport in fractal fields by Neuman [1995], Rajaram and Gelhar [1995], and Di Federico and Neuman [1998] are included.

None of the plumes demonstrate asymptotic or Fickian-type growth, a result that agrees with the analytic theories, as the plume size never exceeds the scale of the largest heterogeneities present. *Rajaram and Gelhar's* model seems to be the best fit for the largest transverse Hurst coefficient ($H_{\text{vert}} = 0.7$). All ensemble results that employed a lower transverse Hurst coefficient ($H_{\text{vert}} = 0.1-0.5$) seem to follow a Mercado-type plume growth. None of the results follow *Di Federico and Neuman's* permanently pre-asymptotic growth.

SUMMARY

We find that the mixing measure $M(\theta)$ has a less significant impact on plume evolution when compared with the effects of variation in the transverse Hurst coefficient. The matrix stretching of the convolution kernel according to the anisotropy of the orthogonal Hurst coefficients has a very significant impact on the continuity of high and low K material within the aquifer. Lower values of the transverse Hurst coefficient lead to greater stretching of the convolution kernel in the horizontal, creating a much more stratified aquifer that exhibits both earlier and later breakthrough. In all of the realistic cases $H_{\text{vert}} < H_{\text{horiz}}$ the plumes demonstrate

nearly Mercado-type growth. Because there is no fractal cutoff in the fBm fields, the plumes never transition to Fickian or asymptotic growth, but always remain in a pre-asymptotic state.

REFERENCES

- Benson D. A., M. M. Meerschaert, B. Baeumer, H.-P. Scheffler, 2006. Aquifer operator scaling and the effect on solute mixing and dispersion, *Water Resour. Res.*, 42(1).
- Castle, J. W., F. J. Molz, S. Lu, and C. L. Dinwiddie, 2004. Sedimentology and fractal-based analysis of permeability data, John Henry member, Straight Cliffs formation (upper Cretaceous), Utah, U.S.A., *J. Sediment. Res.*, 74(2), 270–284.
- Di Federico, V., and S. P. Neuman, 1998. Transport in multiscale log conductivity fields with truncated power variograms, *Water Resour. Res.*, 34(5), 963–974.
- Liu, H., and F. Molz, 1997. Multifractal analyses of hydraulic conductivity distributions, *Water Resour. Res.*, 33(11), 2483–2488.
- Mason, J. D., and Y. M. Xiao, 2001. Sample path properties of operator-self-similar Gaussian random fields, *Theory Probab. Appl.*, 46(1), 58–78.
- Neuman, S. P., 1995. On advective transport in fractal permeability and velocity fields, *Water Resour. Res.*, 31(6), 1455–1460.
- Rajaram, H., and L. Gelhar, 1995. Plume-scale dependent dispersion in aquifers with a wide range of scales of heterogeneity, *Water Resour. Res.*, 31(10), 2469–2482.